International Journal of Recent Technology and Engineering (IJRTE)
ISSN: 2277-3878, Volume-8 Issue-5, January 2020

Deformational Assessment of Shallow Footings Founded on Carbonate Sand

Hossam Eldin A. Ali

Abstract: ***Carbonate (calcareous) sandy soils are well known to be prone to crushability and to have higher compressibility compared to siliceous sands. This study assess the deformational behavior of carbonate (calcareous) sand under shallow footings by carrying out back analyses load tests of twelve full-scale footings founded on improved carbonate (calcareous) sand fill and uniformly loaded up to the allowable bearing pressure. The footings are reinforced concrete isolated pads ranging from 1.5×1.5 m up to 3×3 m in size. These full-scale loading tests are combined with extensive in-situ static cone penetration tests carried out under the location of each footing to test the foundation soil. The recoded measurements of these full-scale load tests are utilized to measure the immediate settlements of the sand fill under variable stresses and to extrapolate long-term (creep) settlement as wells.***

Based on the analyzed results, comprehensive back analyses were carried out to validate several commonly-used settlement prediction formulae, including Schmertmann's method (Schmertmann et al., 1978) and Meyerhof (1965 and 1974) for utilization validation with carbonate (calcareous) coarse-grained materials.

Keywords**: *CPT, Calcareous Sand, Carbonate sand, Settlement, shallow Foundations, Schmertmann method.***

I. INTRODUCTION

Evaluations of the deformation characteristics for vibro-compacted carbonate (calcareous) sand layers are rather difficult and controversial due to the different types, origin, and compositions of the calcareous sand [1]. The carbonate (calcareous) sand fills are usually the main materials used in the reclamation projects in many regions, including the Arabian Gulf, Australia and coral islands, such as in the Maldives and the new Red Sea shore developments.

In this study, a testing campaign comprised several zone load tests (ZLT) performed on reclaimed lands, as part of the ground improvement quality control, were used for this purpose. All these ZLTs were combined with extensive in-situ CPTu tests carried out under the location of each footing before the load testing.

The collection of zone load tests was carried out from several sites located offshore Dubai, Abu Dhabi in UAE as well as from Oman shoreline. The results were used to evaluate the deformational behavior of carbonate sand whether for immediate settlement or long-term creep settlement and validate some of the mostly used settlement prediction formulae for granular soils.

II. CARBONATE SAND DEFORMATIONAL BEHAVIOR

The carbonate sand from the Arabian Gulf is biogenic carbonate sand, which is generally composed of elongated particles with an angular shape and substantial intra-particle voids, which determine, at the macro-scale, a loose structure with a high void ratio [1]. When compressed or sheared, the structurally weak and very angular particles exhibit usually crushing [2], from micro– crushing of the edges to the full breakage of the grains due to the relative weakness of materials with carbonate composition and thin walls and hollow particles. The relatively higher void ratio and crushability of particles leads to a pronounced higher compressibility particularly at higher bearing pressures. In other words, The irreversible plastic strains, the soil undergoes through breakage, result in very low gradient of both the un-loading and re-loading lines.

Although carbonate sands are likely to be crushable, such crushing effects might not be problematic for the use as fill material under relatively low bearing stresses commonly encountered under shallow footings. On the other hand, due to the high-stress level induced by the cone penetration during cone penetration tests (CPT), crushing may cause the carbonate sand to cause lower penetration resistance than quartz or silica sands at comparable densities and stress levels[2] [3]. For this reason, many researchers have introduced correction factors (such as shell correction factors) to be applied to the standard correlation formulas for silica sands [3].

These fixed multiplication factors, which have to be applied to the cone resistance before being applied in any common correlations to estimate some soil parameters or characteristics such as the relative density, elastic modulus, shearing angles, etc. However, several researchers [1][4][5] had denounced such approach proving that the variation of CPT cone resistance between carbonate sand deposits and silica sands cannot be represented by a constant value but rather by nonlinear functions which vary depending on the type of sand involved, relative density, degree of saturation and stress level. Ref. [1] has demonstrated that the difference in behavior between silica and carbonate sand using calibration chambers fit into a centrifuge machine with further confirmation of supplementary tests in a large and conventional calibration chamber using sand taken from one of the offshore borrow areas used to source sand materials used in this study.

Manuscript published on January 30, 2020.
* Correspondence Author
Hossam Eldin A. Ali*, Associate Professor, Department of Geotechnical, Structural Engineering , Faculty of Engineering, Ain Shams University, Egypt.

III. TESTING PROGRAM

The testing program comprised twelve ZLTs form four separate sites. The first site comprises five full-scale foundation models 3×3 m in size, with applied bearing stresses ranging from 50 kPa to 400 kPa. The five foundation models are founded on vibro-compacted carbonate (calcareous) sand fill in two artificial islands reclaimed offshore within the marine territory in UAE, these two islands are denoted here as S1and S2. Three tests in the first island (S1) and two tests in the other island (S2) were conducted, where immediate settlements were measured of each footing at variable stresses. Creep deformation (secondary settlement) was also measured. Similarly, the second and third sites are two reclaimed bodies nearshore of Dubai and were denoted as ISL and PLM. Two zone load tests were carried out on each site. The two tests in the ISL site were 1.5 × 1.5 m square footing while in the PLM site, the size of footing was 2.0 × 2.0 m. Finally, the fourth site located in Al Wusta Province in Oman included three tests carried out on a reclaimed ground with 3.0 × 3.0 m size footings and denoted as OM sites. Each test included several load steps and different loading times as outlined in **Table 1**, with the measured settlement under these various stress levels were recorded. Further details of all testes are also summarized in **Table 1**.

Table 1: Main characteristics of zone load tests

Site	S1&S2	ISL	PLM	OM
Footing Dimensions (m)	3.0 × 3.0	1.5 × 1.5	2.0 × 2.0	3.0 × 3.0
Design Bearing Pressure (kPa)	200 kPa	200 kPa	200 kPa	150 kPa
Test Maximum Pressure (kPa)	400 kPa	600 kPa (300 %)	400 kPa (200%)	187 kPa (125%)
Ground conditions	15 m deep reclaimed carbonate sand overlain bedrock	10 to 15 m deep reclaimed carbonate sand overlain bedrock		6 m of reclaimed carbonate sand overlain marine siliceous sand deposits
Ground improvement	Vibro-compaction with 3.0m grid spacing	Vibro-compaction with 4.0m grid spacing	Vibro-compaction with 3.8m grid spacing	Deep Dynamic Compaction
Test Arrangement	Steel Kentledge, Concrete Blocks, 4 Dial gauges	Steel Kentledge, Concrete Blocks, 4 Dial gauges	Steel Kentledge, Concrete Blocks, 4 Dial gauges	Steel Kentledge, Concrete Blocks, 4 Electronic settlement gauges
Total Test Duration (including Unloading)	11 Days	49 Hours	62 Hours	56 Hours
Main ZLT Loading Stages	100 kPa: 12 Hours	100 kPa: 2 Hours	100 kPa: 2 Hours	112 kPa: 2 Hours
	200 kPa: 12 Hours	200 kPa: 6 Hours	200 kPa: 6 Hours	187 kPa: 48 Hours
	400 kPa: 7 Days	400 kPa: 6 Hours	400 kPa: 6 Hours	-

The actual immediate and creep settlement measurements from the twelve ZLTs were used in this study, after being corrected and interpolated, to carry out back-analyses to verify two commonly used immediate settlement formulae.

Among the different tests loads (bearing pressures stages) done in this testing campaign, certain levels of stresses denoted as first, second and third bearing stress levels or σ_1, σ_2 *and* σ_3, respectively, were considered in this study, as depicted in Table 2.

Table 2 Selected bearing stress levels in this study for each ZLT

Site	ID	First Bearing Stress Level (σ_1) [KPa]	Second Bearing Stress Level (σ_2) KPa]	Third Bearing Stress Level (σ_3) [KPa]
S1	T1	100	200	-
S1	T2	100	200	400
S1	T3	100	200	400
S2	T1	100	200	400
S2	T2	100	200	400
PLM	T1	100	200	400
PLM	T2	100	200	400
OM	T1	122.5	188	-
OM	T2	122.5	188	-
OM	T3	122.5	188	-

IV. IMMEDIATE SETTLEMENT ESTIMATION

There are numerous established methods to calculate immediate settlement for coarse-grained materials [12]. Due to the difficulties of obtaining undisturbed samples for these granular soils, most of these techniques are based on empirical or semi-empirical formulae that correlate settlement directly to in-situ tests, such as SPT, CPT, pressuremeters, etc. Since the development of these methods was typically based on in-situ testing data carried out mainly for silica sands, utilizing these methods for calcareous sand was always extensively disputable. For this reason, re-calibration and validation of these methods in predicting immediate settlement of calcareous sands are verified in this study. Among these methods, two of the most used techniques namely, Meyerhof (1974) [7] and Schmertmann et al. (1978) [8] were considered hereunder for the above-mentioned target.

A. Schmertmann (1970) Strain Factor Method

This method adopted by [8] was initially proposed in 1970 [11] and revised in 1978 [8]. The Schmertmann's method [8] was established to be used for strip and spread shallow footings founded on granular soils. This method considers time effects and correlates elastic modulus E versus CPT cone tip-resistance q_c. This method was developed considering field and model observations and is widely used in practice today to estimate average settlement under the center of rigid shallow footings.

Among other researchers, [13] highlighted that Schmertmann's method is typically conservative (overestimates settlement). According to [14], this method was developed for normally consolidated sand, generally conservative if sand is preloaded or compacted.

Nevertheless, this method is yet one of the most used techniques to calculate the immediate settlement S_e using the following formulae:

$$S_e = C_1 C_2 C_3 \Delta P \sum_{i=0}^{i=n} \frac{I_{zi}}{E_{si}} \Delta Z \quad (1)$$

Where C_1 is a correction factor for the depth of embedment of the footing.

$$C_1 = 1 - 0.5 \frac{\sigma_o'}{\Delta P} \geq 0.5 \quad (2)$$

C_2 is a correction factor for secondary creep settlement

$$C_2 = 1 + 0.2 \log\left(\frac{t}{t_o}\right) \quad (3)$$

t_{yrs} = time since application of load (year) (t ≥ 0.1yr)

C_3 = shape correction factor = 1.03-0.03L/B ≥ 0.73

ΔP is the net increase of foundation bearing pressure at the bottom of the footing = (q - σ'_0)

σ'_0 is the effective stress at footing bottom level before any excavation

I_Z = Strain influence factor at mid-height of each sublayer from idealized strain influence (distribution) proposed in Fig. 1 (non-dimensional)

q_{ci} is the CPT cone tip resistance with an average value assigned to each sublayer.

ΔZ = height of each sublayer.

Ref. [8] modified the strain influence diagram in which the axisymmetric and plane strain loadings were differentiated. Furthermore, the strain influence factor extended to a depth equal to 2B for axisymmetric and 4B for plane strain conditions, as depicted in Fig. 1.

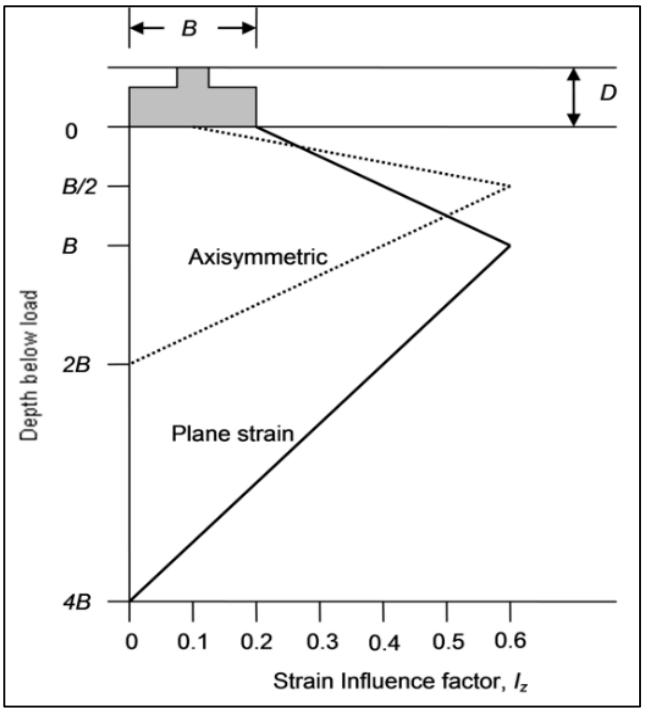

Fig. 1 Proposed Strain influence factors after [6].

Where B is the smallest length of the footing. Ref. [8] also recommended that elastic modulus E_s related to q_{ci} using the following equation:

$$E_s = K_s \times q_{ci} \quad (4)$$

K_s = 2.5 for axisymmetric footings with L/B = 1

K_s = 3.5 for strip footings with L/B > 10

A. Meyerhof (1974) Method [7]

Meyerhof's (1956 [15], 1965 [6] and 1974 [7]) method is a quick and conservative estimation of immediate settlement. The latest version of this approach [7] used the results of twenty case histories to validate this formula shown in (5).

$$S_e = \Delta P \, B / E_s \quad (5)$$

Where, $E_s = K_M \times q_{ci}$, as proposed by [7].

q_{ci} = average static cone resistance within a soil depth equal to B and K_M was proposed to equal 2 according to [7].

Later, [16] updated the K_M to be equal 1.5 for silt and sand, 2 for compacted sand, 3 for dense sand, and 4 for sand and gravel.

V. SAND LONG-TERM (CREEP) SETTLEMENT

A. Soil Creep according to Briaud and Garland method

The creep rate can be estimated based on the model proposed by [17]. This method allows predicting the time-dependent behavior of all soils. This creep model considers the following formula in (6) to represent creep behavior of granular soils:

$$\frac{S}{S_1} = \left(\frac{t}{t_1}\right)^n \quad (6)$$

Where S is the measured settlement at time t from the application of the incremental load step counted from the beginning of the initial loading, the settlement S_1 is the value of S corresponding to a time t_1. The time t_1 is considered in all tests to be at 1.0 min after the beginning of every load-step as suggested by [17]. However, [18] adopted 30 min for time t_1. It was noted by the Author that initial time may vary depending on the type of formations (soil foundation) and the applied bearing stress, however 20 to 30 min for t_1 was adopted for all ZLTs under bearing stress exceeding 100 kPa, while 1.0 minutes proved to provide better results for low bearing stress at 100 kPa or less.

Finally, n is the time exponent, a property of the soil as indicated by [17], with a range typically vary from 0.005 to 0.03 for silica sand as suggested by [18].

In order to find n value at each loading step, the time-settlement data have to be plotted as $log\ S/S_1$ versus $log\ t/t_1$; as such, the slope of the linear regression line would equal n.

B. Soil Creep according to Schmertmann method

Another approach of estimating creep behavior is to use the C_2 parameter, as indicated by [7] and included in (3). It was suggested by [7] that t_o to be about one month (0.1 year) while Euro-Code 8 Part 2 [20], implicitly proposed to have t_o to be one year. According to the latter suggestion, C_2 would equal 1.2, 1.26 and 1.34 for 10, 20 and 50 years of creep, respectively comparing to the value of 1.4, 1.46 and 1.54 suggested initially by [7] for the same time intervals.

VI. TESTING DESCRIPTION AND METHODOLOGY

A. Full-scale tests description

Twelve zone load tests were conducted to measure immediate settlements and to extrapolate long-term settlements of reclamation fill of several reclamation islands/lands under various bearing pressures.

Each test consists of a bearing square slab from 1.5 m to 3 m width. In all tests, the tested slab was loaded by a hydraulic jack; the bearing slab is placed on cement stabilized sand. Kentledge with different configuration was used as a reaction weight for all the considered test as schematically depicted in Fig. 2 and shown in the sample photo in Fig. 3.

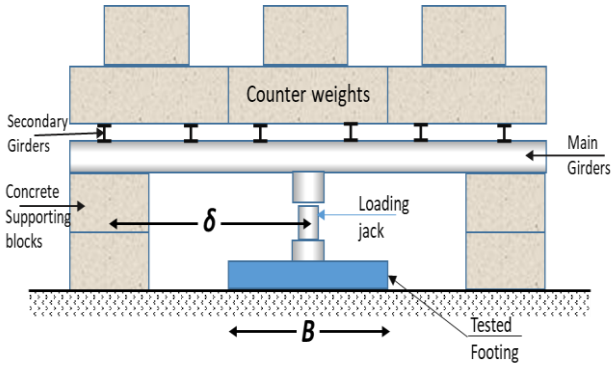

Fig. 2 Schematics of the typical zone load test setup

A steel reference frame with a span ranged from 9.0 m to 12 m was used. This frame was founded on a steel supporting frame. One side of the measuring frame was fixed to the steel supporting frame while the other side was on sliding support to avoid thermal-induced stresses in the frame elements due to temperature changes. The reference frame was protected from hot weather conditions through a tarpaulin. The measurements were recorded manually and, in some tests, utilizing an automatic data logger system able to collect data in 1.0-minute increments during the entire test. However, in some tests due to the malfunction of the data logger, manual reading was taken.

The elevation and leveling of the settlement plate, kentledge foundation, and reference frame foundation were checked by means of optical leveling to a fixed datum. These measurements were performed before the commencement of each ZLT, before increasing the intermediate load steps and finally after the completion of the test.

Finally, the settlement was measured as the average reading of four transducers placed at the corners of each footing/pad.

Fig. 3 Photo for zone load test setup for site S2

B. Sand Fill Materials

The fill materials used in all sites considered in this study are mainly calcareous sand with carbonate content mainly exceeding 88% obtained from offshore borrow areas utilizing marine dredging operations. Table 2 provides the main properties of the fill material.

Table 2: Overview of the lab test results for the sand fill

Parameter	Unit	S1 & S2	PLM & ISL	OM
Average particle size (D_{50})	[mm]	0.23-0.8	0.23-0.66	-
% smaller than 75µm	[%]	2.0 -3.0	1.0 -11.0	4.0-8.0
Carbonate content	[%]	93-95	88-94	91-94
Min. dry density	[kN/m^3]	10.9- 12.2	-	13.6-14.7
Max. dry density	[kN/m^3]	14.1-16.0	-	16.6-17.1

Further details regarding the lab testing program for typical sand used particularly as fill materials in S1 and S2 sites and difficulties in testing crushable sand are presented in Wils et al. (2013) [21]. In another comprehensive study, [5] provided state-of-art analyses and lab results of the same sand used in S1 and S2 sites.

C. Tests Results

The results of the performed zone load tests (settlement versus load or settlement versus time) were recorded. Fig. 4 and Fig. 5 show the deformation as a function of applied stresses (settlement vs. load) for all the considered ZLTs and Fig. 6 shows the relation between the recorded settlement and time for S1 and S2 sites over an extended loading period up to 24 days. Similarly, Fig. 7 shows the same results for ISL, PLM and OM sites but for shorter loading periods limited to maximum three days only.

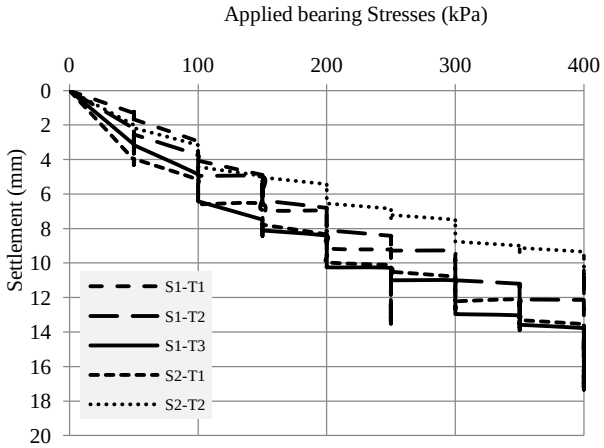

Fig. 4 Settlement versus load from Sites S1 and S2

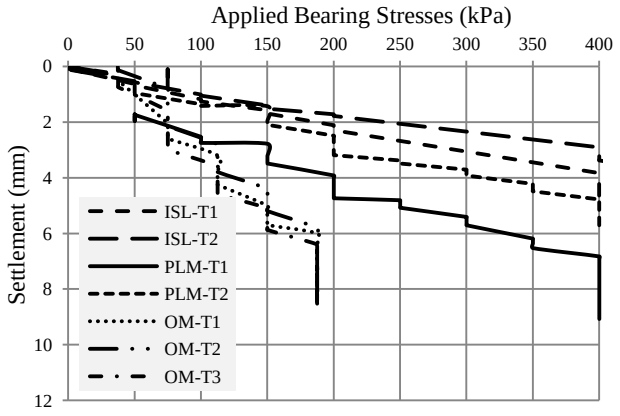

Fig. 5. Settlement versus load from Sites ISL, PLM and OM

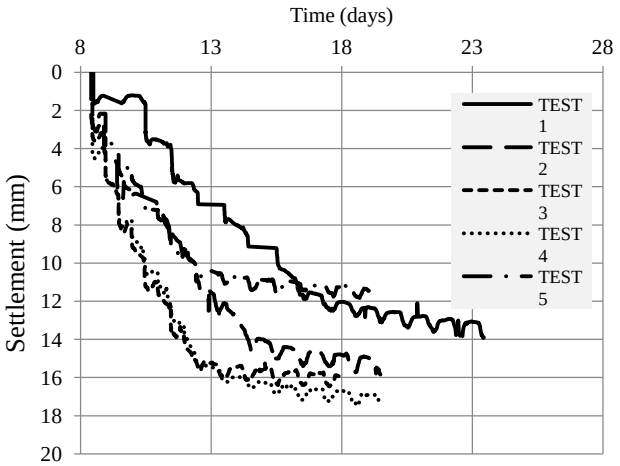

Fig. 6. Settlement versus time from Sites S1 and S2

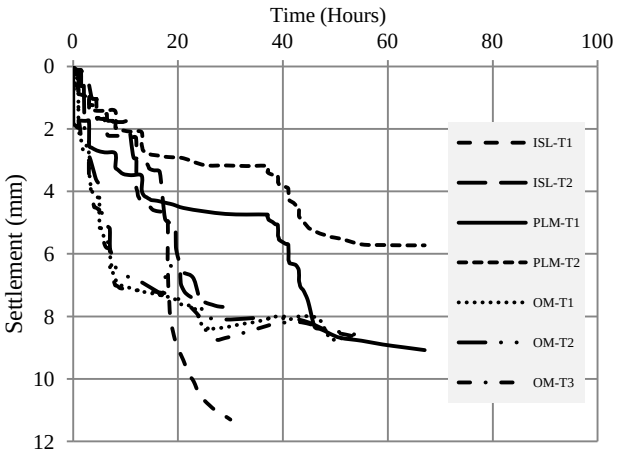

Fig. 7. Settlement versus time from Sites ISL, PLM and OM

D. CPTu testing

All ZLTs were carried out after conducting several CPTu at the location of each test. The representative CPTu location and orientation of the load plate compared to footing for the first five tests are shown in Fig. 8.

Each CPTu pair tests consists of two points *a* and *b*, performed in between the vibro-compaction probes as shown in **Fig. 8**. Fig. 9 presents the pair CPTu cone tip resistance q_c and their averages for S1-T1 and S1-T2 as a typical example while the average q_c for all ZLT areas are presented in **Fig. 8**.

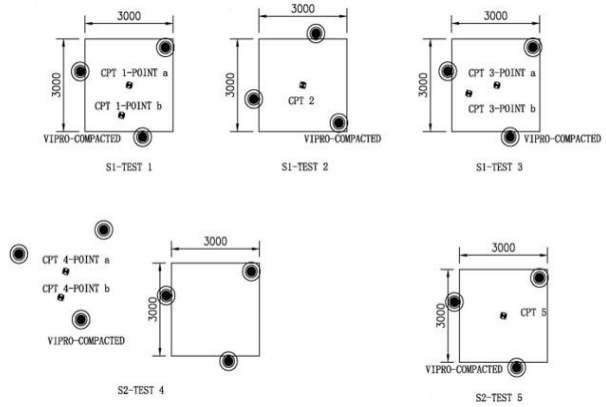

Fig. 8. Plan View of the footings in relation to CPT soundings locations and vibro-probes locations for tests in S1 and S2 sites

VII. BACK ANALYSES METHODOLOGY

In order to carry out reliable back-analyses of the measured raw data, several adjustments and corrections were adopted to relate the measured settlement to the calculated ones. These measures had accounted for the test setup effect, CPT repeatability and variability effect as well the spatial variability of the tested soil layers. These measures included:

i. Corrections for soil strengthening due to confining pressure by the load reaction platform effect;
ii. Using a representative average value of the cone resistance (q_{c-av}) over the influence depth to account for ground variations with depth; and
iii. Estimate a best-fitting unified relationship between the measured immediate settlement (S_{em}) and CPT cone tip resistance (q_{c-av}) over each test location, in order to estimate a modified settlement values (S_{em-fit}) through interpolation using the resulted curve. This step was needed to account for CPT test repeatability and spatial variation in ground condition along each site.

The following sections explain in detail the methodology and steps used to account for inherited variabilities and errors associated with the tests setup as well as with the test results and compacted soil conditions.

A. Correction methodology of measured settlement due to Load Reaction Platform

As shown above, all tests were performed using a reaction platform (kentledge), as shown in **Fig. 2**. The blocks supporting the platform induce bearing pressure on the ground. Such pressure causes a strengthening of soil underneath the tested pad due to both confining and preloading effects.

Accordingly, the measured settlement values from ZLTs are typically underestimated due to the strengthening (confining) effect of the support bearing stresses particularly for lower tested bearing stresses. Therefore, the actual measured immediate settlement (S_e) under each footing needed to be corrected for this effect.

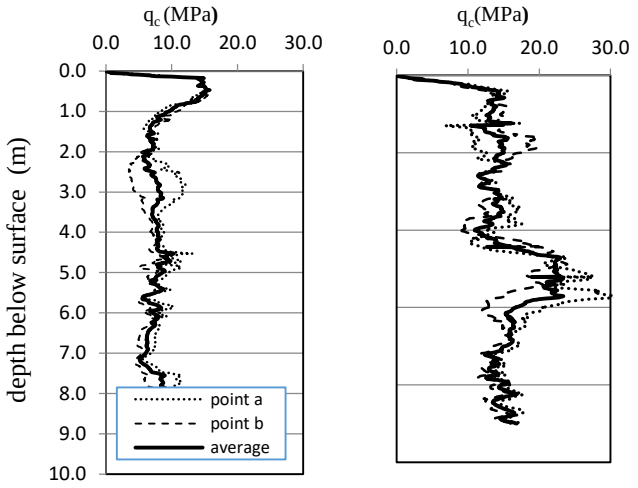

Fig. 9. CPTu cone tip resistance profiles for S1-T1 (left profile) and S1-T2 (right Profile)

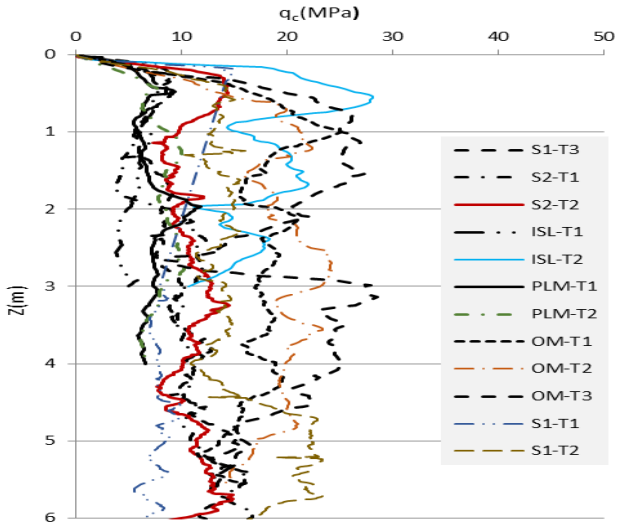

Fig. 10. CPTu cone tip resistance average profiles for all tested plots [Note: q_c values are shown only down to depths up to three times the width of the footing (B)]

In this study, the measured immediate settlement (S_e) under each footing were corrected at the three main bearing stress levels (σ_1 , σ_2 *and* σ_3) listed in Table 2. The corrected settlement S_{em} was obtained by using correction factor (C_{RP}), so that:

$$S_{em} = C_{RP} \times S_e \qquad (7)$$

For this purpose, several 3D finite element models were carried out using PLAXIS 3D to simulate the test setup conditions, at each stress level, for the four main sites. By comparing the settlements S_N (as in **Fig. 13** (a)(c)) induced under the main testing footing considering the confining stresses by the kentledge bearing blocks against the settlements S_{NB} induced under the main testing footing only (as in **Fig. 13** (b)(d)), an estimation of the correction factors C_{RP} at each applied bearing pressure were developed as shown below in Table 3 to Table 6 for S1 & S2, ISL, PLD, and OM sites, respectively.

Accordingly, a corrected measured settlement (S_{em}) were estimated by multiply the measured settlements by the corresponding correction factor (C_{RP}) as indicated by (7).

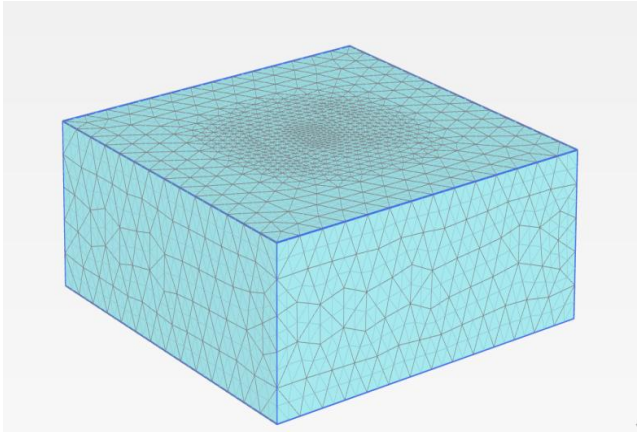

Fig. 11. Plaxis-3D finite element mesh used in the analyses

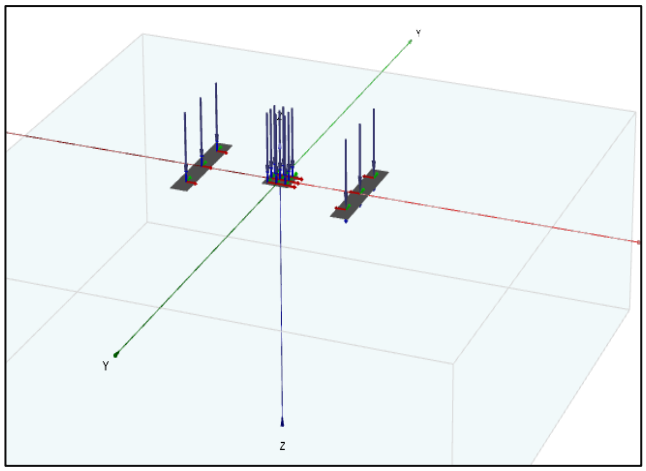

Fig. 12. Plaxis-3D loading footprint on the model surface in 3D view

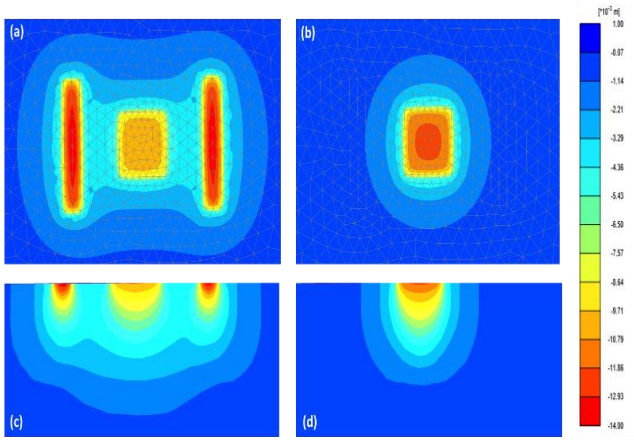

Fig. 13. PLAXIS-3D deformation results for S1-T1 at stress 100 kPa. (a) & (c) Plan and sectional views for maximum deformation for model with reaction supports (blocks); (b) & (d) Plan and sectional views for maximum deformation for model without reaction supports (blocks)

Table 3: Correction factor due to load reaction platform for each load for S1 and S2 sites

Testing Bearing Pressure (kPa)	S_N (mm) Considering Blocks	S_{NB} (mm) Neglecting Blocks	Correction factor (C_{RP})
100	7.18	12.33	1.72
200	13.64	22.97	1.68
400	29.58	44.8	1.51

Table 4: Correction factor due to load reaction platform for each load for ISL sites

Testing Bearing Pressure (kPa)	S_N (mm) Considering Blocks	S_{NB} (mm) Neglecting Blocks	Correction factor (C_{RP})
100	6.90	8.68	1.258
200	13.40	17.21	1.286
400	28.32	34.19	1.207

Table 5: Correction factor due to load reaction platform for each load for PLM sites

Testing Bearing Pressure (kPa)	S_N (mm) Considering Blocks	S_{NB} (mm) Neglecting Blocks	Correction factor (C_{RP})
100	7.82	10.38	1.33
200	14.85	19.42	1.31
400	32.03	38.01	1.19

Table 6: Correction factor due to load reaction platform for each load for OM sites

Testing Bearing Pressure (kPa)	S_N (mm) Considering Blocks	S_{NB} (mm) Neglecting Blocks	Correction factor (C_{RP})
122	6.65	9.33	1.4
188	13.97	16.78	1.20

B. The averaging of the q_{ci} measurements

As depicted in **Fig. 10**, the measured CPTu tip resistance (q_{ci}) beneath or nearby the footprint of the test footings might vary significantly with depth. Therefore, different averaging approaches were applied to get a representing average q_{ci} over the influencing zone or depth under each footing. The first approach is the weighted harmonic mean (WHM) using (8) and the other approach is the Linearly Weighted Moving (LMW) Average using (9).

$$q_{c.av1} = \frac{((n)+(n-1)+(n-2)+\cdots)}{(\frac{n}{q_{c1}} + \frac{n-1}{q_{c2}} + \frac{n-2}{q_{c3}} + \cdots)} \quad (8)$$

$$q_{c.av2} = \frac{(q_{c1}(n) + q_{c2}(n-1) + q_{c3}(n-2) + \cdots)}{((n)+(n-1)+(n-2)+\cdots)} \quad (9)$$

Where *n* is the segment number counted from the bottom of the footing down to the investigated depth (*Z*).
Both methods weight the closer-to-footing CPT cone measurements more heavily than farther (deeper) ones using different weights. In this regard, two influence zones or depths (*Z*) below each footing were investigated; One equal to the width of the loading pad (i.e. Z = B) and the second is twice the width of the loading pad (i.e. Z= 2B). Based on the fitting analyses carried out, it was concluded, in general, that $q_{c.av}$ using the LMW method over influence depth of 2B is the best approach to cater for ground variation in the vertical direction and hence was used in all subsequent analyses. It is important to note that this finding was not necessary to apply to all cases studied.

C. Site-specific best-fitted methodology

Due to the spatial variability of the improved granular fill material and the measured q_c under each footing over each site, a best fitting relation (S_{em-fit}) between (S_{em}) and $q_{c.av}$ were drawn for each site, as shown in **Fig. 14** which depicts the best fitting curves for site S1 at bearing stress of 100 kPa considering averaging over 1B and 2B. A similar procedure was carried out to develop the best fitting curve for each stress level at each site. Accordingly, a modified settlement value (S_{em-fit}) for each test was calculated. Table 8 to Table 10 lists the modified settlement values (S_{em-fit}) for all tests at the first, second and third bearing stress levels, respectively. Such values were used for back analyses of each settlement prediction formulae.

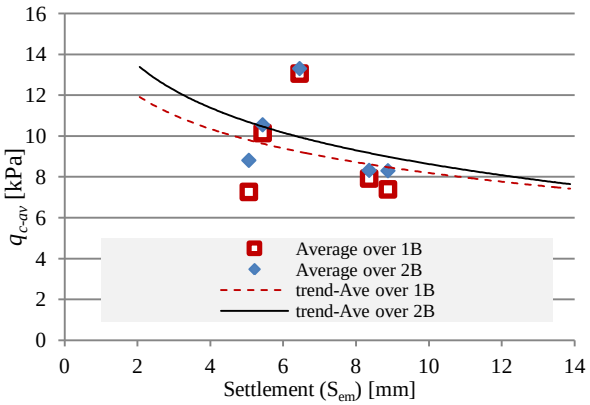

Fig. 14. Settlement S_{em} versus q_c under 100 kPa for site S1

Table 7: Average $q_{c.av}$ over an influencing depth equal to B, 2B below the footing using two average methods

Site	ID	$q_{c.av1}$ (MPa) within Z=B WHM method	$q_{c.av2}$ (MPa) within Z=B LMW method	$q_{c.av2}$ (MPa) within Z=2B LMW method
S1	T1	7.26	9.79	8.8
S1	T2	13.05	12.03	13.30
S1	T3	7.91	7.04	8.31
S2	T1	7.38	6.80	8.29
S2	T2	10.14	10.20	10.54
ISL	T1	5.78	6.31	6.11
ISL	T2	16.58	18.34	18.58
PLM	T1	6.91	5.94	6.83
PLM	T2	7.77	6.33	7.46
OM	T1	17.88	15.95	16.96
OM	T2	15.84	15.17	17.74
OM	T3	16.70	19.02	20.14

D. Estimation of allowable bearing capacity of soil

In order to estimate the actual allowable bearing capacity q_{all} of each analyzed footing based on the actual soil condition under each footing,

The calculated average CPT tip-resistance q_{c-av} are employed directly to estimate the allowable bearing capacity. The approach followed methods suggested by [8] and [22] which are typically based on empirically-driven formulae after the back-evaluations of foundation performance. The average value of these two direct methods was utilized hereunder for a square footing as suggested by [8] using (10) and according to [22] using (11).

$$q_{all} = 0.55P_a(q_{c-av}/P_a)^{0.785} \quad (10)$$

$$q_{all} = K_{\emptyset}\, q_{c-av} \quad (11)$$

Where $K_{\emptyset}$ = 0.2 for no embedment after [20] and P_a is the atmospheric pressure. The value of the average q_{all} over a depth equal to *B*, below the footing that has been calculated. Accordingly, the values of q/q_{all} for the twelve ZLTs under various stress levels are listed in Table 11, where q is the actual applied bearing pressure.

Table 8 Modified immediate settlement within Z=2B under the first level of bearing pressure (σ_1)

Site	ID	S_e (mm)	$S_{em.}$ (mm)	S_{em-fit} (mm)
S1	T1	2.94	5.06	6.00
S1	T2	3.75	6.45	4.50
S1	T3	4.86	8.36	8.50
S2	T1	5.16	8.88	9.50
S2	T2	3.16	5.44	5.50
ISL	T1	1.18	1.48	1.48
ISL	T2	1.00	1.26	1.26
PLM	T1	1.36	1.81	1.90
PLM	T2	2.5	3.33	2.00
OM	T1	4.35	6.09	6.09
OM	T2	4.2	5.88	5.88
OM	T3	3.8	5.32	5.32

Table 9 Modified immediate settlement within Z=2B under the second stress level of bearing pressure (σ_2)

Site	ID	S_e (mm)	$S_{em.}$ (mm)	S_{em-fit} (mm)
S1	T1	6.94	11.66	11
S1	T2	6.8	11.42	8
S1	T3	8.42	14.15	15.5
S2	T1	8.33	13.99	16.5
S2	T2	5.43	9.12	10
ISL	T1	2.1	2.70	4
ISL	T2	1.72	2.21	1
PLM	T1	2.49	3.26	4.5
PLM	T2	3.9	5.11	5.46
OM	T1	7.6	9.12	9.12
OM	T2	7.29	8.75	8.75
OM	T3	8.9	10.68	6.00

Table 10 Modified immediate settlement within Z=2B under the third level of bearing pressure (σ_3)

Site	ID	S_e (mm)	$S_{em.}$ (mm)	S_{em-fit} (mm)
S1	T2	12.15	18.35	12.50
S1	T3	13.77	20.79	23.00
S2	T1	13.53	20.43	24.00
S2	T2	9.35	14.12	16.00
ISL	T1	3.79	4.57	4.57
ISL	T2	2.88	3.48	3.48
PLM	T1	4.78	5.69	6.69
PLM	T2	6.89	8.20	6.00

Table 11 q/q_{all} over a depth equal to B below the footing

Site	ID	q/q_{all} for first load stress (σ_1)	q/q_{all} for second load stress (σ_2)	q/q_{all} for third load stress (σ_3)
S1	T1	0.1532	0.3064	-
S1	T2	0.1246	0.2493	0.4986
S1	T3	0.2131	0.4261	0.8523
S2	T1	0.2206	0.4412	0.8824
S2	T2	0.1470	0.2941	0.5882
ISL	T1	0.2375	0.4751	0.9501
ISL	T2	0.0818	0.1636	0.3272
PLM	T1	0.2524	0.5047	1.0094
PLM	T2	0.2368	0.4736	0.9472
OM	T1	0.0941	0.1881	-
OM	T2	0.0989	0.1977	-
OM	T3	0.0789	0.1578	-

VIII. IMMEDIATE SETTLEMENT BACK ANALYSES RESULTS

A. Results and Discussion for Schmertmann Method

Back analysis was undertaken for Schmertmann's method to validate the original suggested value of K_S. by [8]. Accordingly, the new (modified) values or "$K_{S.mod}$" was estimated using (12):

$$K_{S\,mod} = \frac{\text{Calculated settlement.}}{\text{Measured settlement or } S_{em-fit}} \times K_S \quad (12)$$

Schmertmann's method [8] proposed originally the K_S value to be equal to 2.5 for axisymmetric footings under normal siliceous sand. Based on the back-analyses of all tests, the $K_{S.mod}$ estimated values were plotted versus the measured q_{c-av} as shown in Fig. 15 in order to evaluate the impact of relative density (or level of densification) of sand on the $K_{S.mod}$.

The best fit value for $K_{S.mod}$ for Schmertmann was imposed on the same graph shown in Fig. 15. According to Fig. 15, the $K_{S.mod}$ varies between 2.5 for q_{c-av} exceeding 20 MPa to 7.5 when q_{c-av} is being less than 8 MPa. As such, the original K_S values as proposed by [8] can be used whenever the q_{c-av} value exceeding 20 MPa.

These findings controvert with the previously considered facts regarding the impact of the crushability of calcareous sand on CPT measurements particularly at higher q_c values that believed to lead to underestimating the relative density of the soil[1]-[3]. Thereby, the higher the q_{c-av} value, the more underestimation in predicting settlement would be expected by using settlement formulae. Accordingly, it was anticipated that $K_{S.mod}$ to increase with the increase of q_{c-av} to satisfy that effect. However, the observed decrease in the measured $K_{S.mod}$, in Fig. 15, based on actual data was apparently compelled (or compensated) by the impact of the increase of q_{c-av} itself.

It was also observed from Fig. 15 that the actual applied bearing pressure q had no apparent impact on the $K_{S.mod}$ trend. This was also true when using the normalized bearing pressure q/q_{all} categories as shown in Fig. 16.

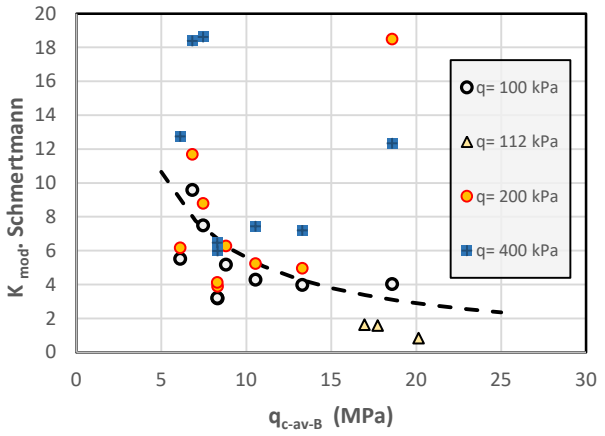

Fig. 15. Schmertmann's (modified) values of K_{mod} against q_{c-av} for different bearing pressure (q) ranges

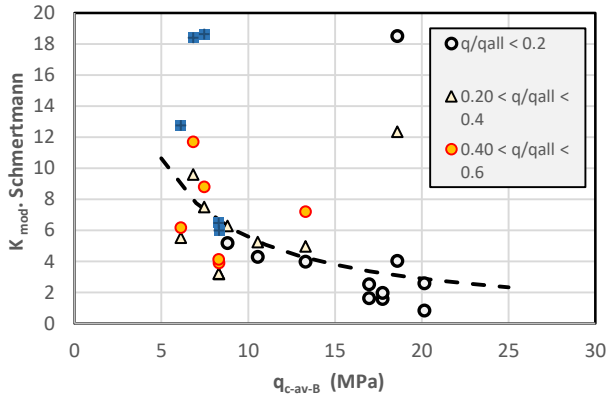

Fig. 16. Schmertmann's (modified) values of K_{mod} against q_{c-av} for different (q/qall)

An alternative approach was used to capture the impact of the level of normalized bearing pressure by considering the impact of the applied level of bearing pressure in relation to the maximum allowable bearing pressure q/q_{all}, on the variation of $K_{S.mod}$. Therefore, the $K_{S.mod}$ was plotted against normalized bearing pressure q/q_{all} as shown in Fig. 17. In this figure, $K_{S.mod}$ proportionally increased from 2.5 for an actual bearing pressure less than 10% of the maximum allowable bearing pressure q_{all} and mounting to the value of 13.0 at a bearing pressure level equal to the maximum allowable bearing pressure $q_{all.}$ (or $q/q_{all} = 1$) as shown in Fig. 17.

In case the data of the sites PLM and ISL are ignored, the extreme value for $K_{S.mod}$ was being limited to 6.3 for an actual bearing pressure approaching to the maximum allowable bearing pressure $q_{all.}$ as depicted in Fig. 18. As such, it is not recommended to consider higher value for $K_{S.mod}$ than 6.0.

Nevertheless, both figures suggest that K_S cannot be a fixed value, as originally suggested by [8]. More importantly, as discussed by [2], the increase in $K_{S.mod}$ with the applied stress can be directly related to the behavior of uncemented carbonate sand (similar to silica sand) that appears to be governed more by the initial void ratio rather than by compressibility of the soil particles. The reduction in void ratio with the increase of confining stress induced by the applied footing bearing pressure causing a strong tendency for the elastic modulus to increase particularly from a moderate range of applied stress as experienced in the conducted ZLTs. In other words, the carbonate sand exhibited a rather typical behavior to the applied stresses similar to silica sand.

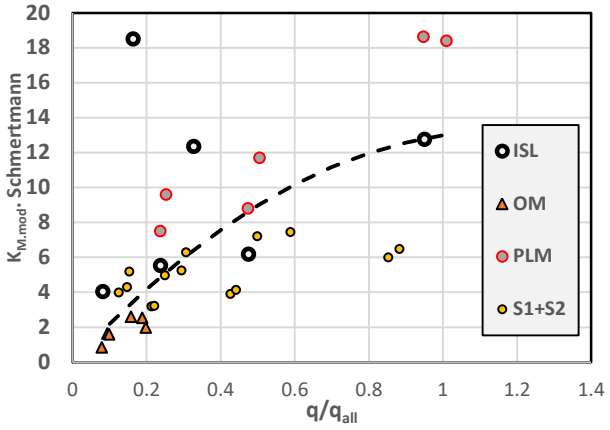

Fig. 17. Schmertmann's (modified) values of K_{mod} against (q/qall) considering all zone load tests

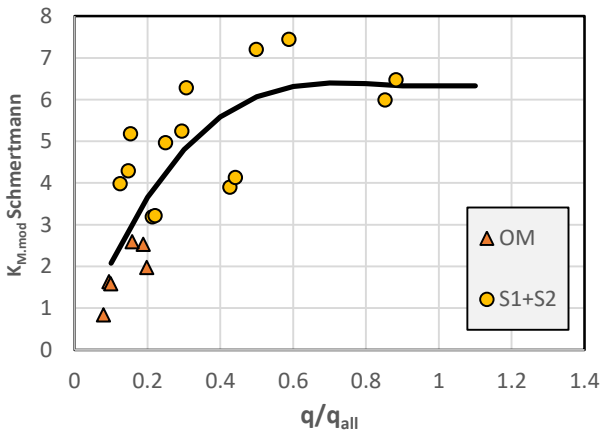

Fig. 18 Schmertmann's (modified) values of $K_{S.mod}$ against (q/qall) for zone load tests considering OM and S1+S2 sites only.

B. Results and Discussion for Meyerhof's Method [7]

Similar to Schmertmann's method approach, a back analysis was undertaken by calculating the settlement using the original Meyerhof's method [7], the new (modified) values of $K_{M.mod}$ have been calculated as in (13):

$$K_{M\ mod} = \frac{\text{Calculated settlement.}}{\text{Measured settlement or } S_{em-fit}} \times K_M \qquad (13)$$

It is to be noted that [7] had assumed the zone of influence is to be equal to the footing width (B) under the footing and as such, K_{org} was limited to 2 (for Compacted sand). So, the $q_{c-av-1B}$ was considered in this particular analyses.

By plotting the $K_{M.mod}$ against the variation of applied bearing pressure to the maximum allowable bearing pressure q/q_{all}, for all sites, as depicted in Fig. 19, it was revealed that $K_{M.mod}$ varied from 5.13 to 14.90 as an actual average value at pressures ranges from 10% to 100% of the q_{all}. The upper range $K_{M.mod}$ is tamed down to 8.5, if only S1, S2 and OM sites were considered as shown in **Fig. 20**.

So similar to Schmertmann's method, the impact of the increasing bearing pressure is evidently causing the values of $K_{M.mod}$ to increase.

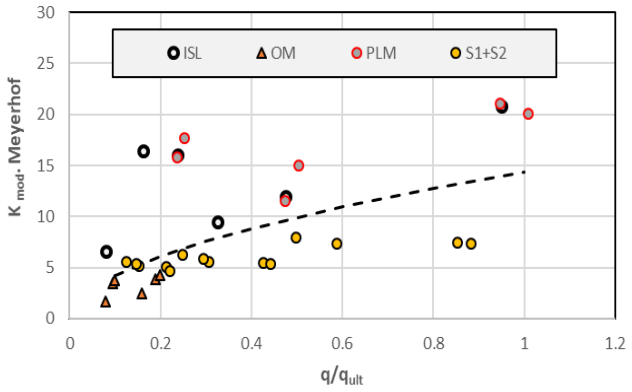

Fig. 19. Meyerhof's [7] modified values of $K_{M.mod}$ against (q/q_{all}) for all ZLTs in all sites

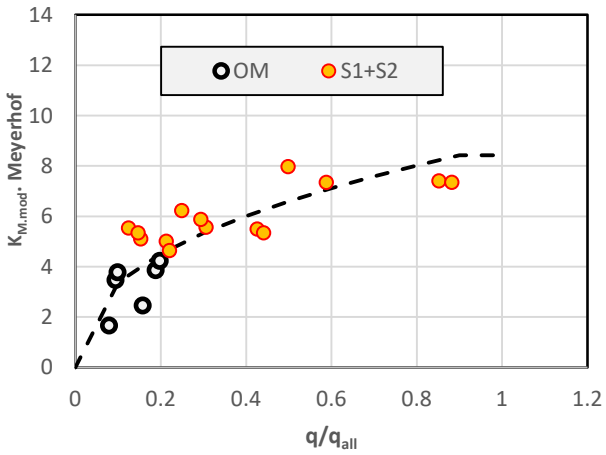

Fig. 20 Meyerhof's (modified) values of K_{mod} against (q/qall) for ZLTs in OM and S1+S2 sites only

IX. CREEP SETTLEMENT BACK ANALYSES RESULTS

A. Results and Discussion for Briaud and Garland method

Back analysis has been done after calculation of the creep exponent *n*, as recommended by [17] [18], for the sites S1, S2, PLD, and OM only.

ISL site was not considered in creep analyses since time allowed for creep to occur at each load step in ISL site was significantly limited (less than 2 hours). Fig. 21 provides a typical sample for the estimation of the exponent *n* value from the creep curves for PLM –T1 at 100, 200 and 400 kPa bearing pressures.

By carrying out similar analyses for all sites, all results were summarized for the considered sites at different bearing stress levels in Table 12.

Based on these results, a collective curve between the exponent *n* value and the normalized bearing pressure (q/q_{all}) is presented in Fig. 22 where the average *n*-value ranges between 0.025 at very low normalized bearing pressures and 0.05 at the allowable bearing pressure (i.e., q/q_{all} = 1.0).

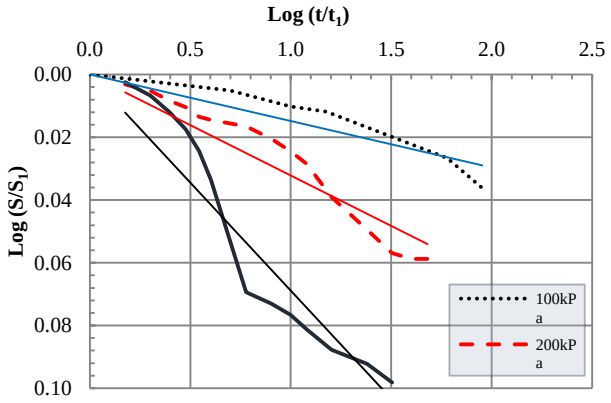

Fig. 21. Creep curves for PLM –T1 for 100, 200 and 400 kPa bearing pressures

Upon studying the effect of the range of average cone tip-resistance ($q_{c.av}$) alone on the time exponent *n* value, it was found that the impact would be insignificant.

However when using a normalized n_m to the foundation width B and the average cone tip-resistance ($q_{c.av}$) as per (14), a better and more significant fitting relation was obtained as shown in Fig. 23.

$$n_m = {}^{n}/_{(B.q_{c.av})} \qquad (14)$$

According to Fig. 23, the n_m value would range from 5×10^{-3} to 2×10^{-2}. In fact, a constant value of 0.001, as an average value, would be a reasonable representing approximation over the full range of bearing pressures up to the allowable bearing pressure (q_{all}).

Table 12 Estimation of Creep coefficient n at different bearing stress levels

Site	ID	n at σ_1	n at σ_2	n at σ_3
S1	T1	0.0297	0.025	-
S1	T2	0.0259	0.0326	0.0391
S1	T3	0.0267	0.0203	0.0235
S2	T1	0.0203	0.0202	0.0246
S2	T2	0.0286	0.0207	0.0303
PLM	T1	0.0148	0.032	0.0688
PLM	T2	0.0096	0.0373	0.0412
OM	T1	0.0282	0.0342	-
OM	T2	0.0214	0.044	-
OM	T3	0.0212	0.0293	-
Average value		0.0226	0.0296	0.0379

Retrieval Number: E6345018520 /2020©BEIESP
DOI:10.35940/ijrte.E6345.018520
Journal Website: www.ijrte.org

Published By:
Blue Eyes Intelligence Engineering
& Sciences Publication

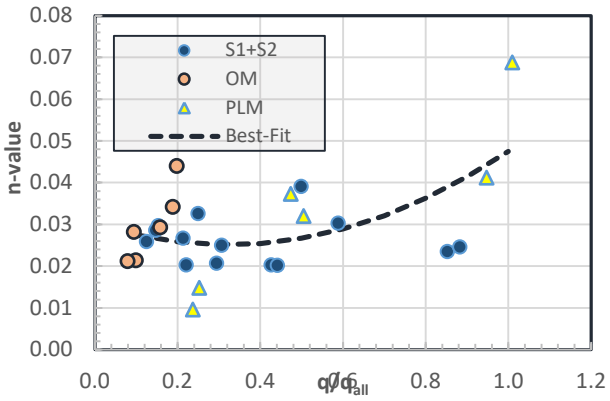

Fig. 22. Creep exponent n value versus the normalized bearing pressure.

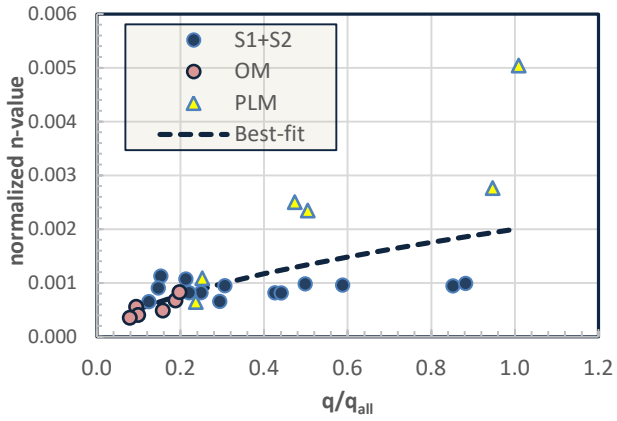

Fig. 23. The normalized creep exponent nm value versus the normalized bearing pressure

B. Results and Discussion for Schmertmann Method [8]

Since the new (modified) values of $C_{2\,mod}$ by [8] can be represented as:

$$C_{2\,mod} = \frac{S}{S_1} = \left(\frac{t}{t_1}\right)^n \qquad (15)$$

Thereby, assuming t = 10, 20 and 50 years and t_1 = one year as recommended by [20] would yield to the following results presented in Fig. 24 where the variation of $C_{2\,mod}$ can be depicted. Based on the average values at allowable bearing pressure the $C_{2\,mod}$ would be equal to 1.12, 1.5 and 1.21 for 10, 20 and 50 years, respectively.

Accordingly, it would be concluded that these parameters are rather closer to the estimation of C_2 as modified by Euro-Code1997 (EC-7) [13].

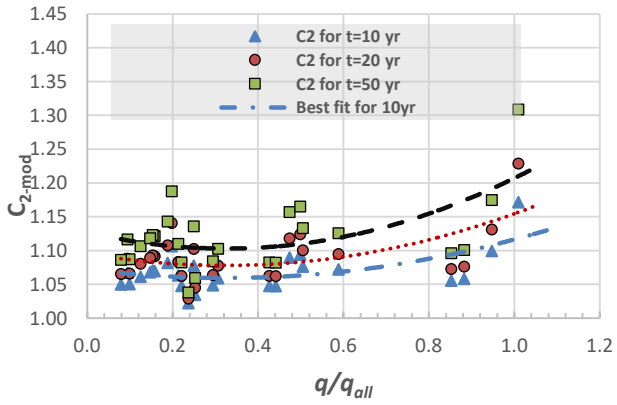

Fig. 24. Schmertmann et al. (1978) creep parameter $C_{2\,mod}$ for time 10, 20 and 50 years versus the normalized bearing pressure.

X. CONCLUSION

This study evaluates the potential difference of deformational behavior of carbonate (calcareous) sands under shallow footings. For this regard, testing data from twelve full-scale zone (footing) load tests conducted on compacted granular carbonate sand materials were utilized to develop specific deformational parameters for carbonate sand for both immediate settlement and long-term creep settlement.

In this study, the correction factor counting for the effect of carbonate sands on the measured CPT values (commonly known as Shell Correction Factor[3]) was not considered; Alternatively, this study evaluates combinedly the effect of calcareous sands crushability against the measured CPT values as well as the compressibility of the carbonate (calcareous) sands under the established bearing pressure. Both effects are inherently combined within one factor noted as K_{mod} relating the raw CPT cone tip resistance to the soil elastic modulus, for Schmertmann [8] or Meyerhof [7] formulae.

For immediate settlement estimation for shallow footing on granular sand using [8] and [7], there was a clear difference between the predicted settlement using commonly settlement formulae utilizing their own original parameters and the site-specific parameters or (K_{mod}) developed in this study.

The results back analyses suggested that both methods considered in this study are utilizing low K value that tends to overestimate the predicted immediate settlement. This matching the findings of [13] and [14] for silica sands. Accordingly, the observed behavior under the ranges of applied stresses cannot directly be related to the crushability or compressibility of the carbonate sand.

More interestingly, it was concluded that these parameters, for both prediction methods, are rather variable and depending on the stress level applied and strength of the soil.

In both prediction methods, the back-analyses was limited to q/q_{all} less than 1.0 with the heaviest cluster of data was for results of q/q_{all} less or equal 0.6. As such, for carbonate materials, it is recommended to consider in predicting the immediate settlement, a direct correlation factor K_{mod} as presented in Fig. 18 for Method [8] and Fig. 20 for Method [7] using raw cone-tip resistance values obtained from the CPT test up to a value of $q/q_{all} = 0.6$.

On the other hand, despite the potential higher compressibility of carbonate sand, the conducted ZLTs, in general, did not show any significant evidence that carbonate sand might undergo under higher creep rates than silica sand. In fact, the results collected from this study suggested that similar creep rates as suggested by Eurocode -7 [20] can be adopted for carbonate sand.

Finally, it is essential to note that the main findings of this study were merely to demonstrate and highlight the deformational behavior of carbonate sand based on actual measurements and such findings must not be used directly in design unless further independent verifications are conducted. Moreover, the findings of this study shall be limited to the range of bearing pressures and sizes of the considered footings as well as the type and density of soils tested for these methods, and hence cannot be generalized to other soils or foundations types.

The loading periods for testing creep were rather over a short period and hence the extrapolation to very extendable periods such as 50 years would be taken cautiously unless longer long-term validation is carried out. However, such results shall be considered as a valid indication of the expected long-term deformation of shallow footings.

REFERENCES

1. D. Giretti, K. Been, V. Fioravante and S. Dickenson. (2017) CPT calibration and analysis for a carbonate sand. Géotechnique, Vol 68, Issue 4. [http://dx.doi.org/10.1680/jgeot.16.P.312].
2. T. Lunne, "Guidelines for use and interpretation of CPT in hydraulically constructed fills," NGI Report 20041367-3, 2006.
3. A. S. Al-Homoud and W. Wehr "Experience of vibrocompaction in calcareous sand of UAE," Geotechnical and Geological Engineering (2006) 24: 757–774. DOI 10.1007/s10706-005-1707-8 .
4. H. G. Poulos, "The Mechanics of Calcareous Sediments, John Jaeger Memorial Lecture," Australian Geomechanics, Special Edition, (1988) 8-41.
5. D. Giretti, V. Fioravante, K. Been, and S. Dickenson, "Mechanical properties of a carbonate sand from a dredged hydraulic fill," Géotechnique, Vol 68, Issue 5, 2017. [https://doi.org/10.1680/jgeot.16.P.304].
6. G. G. Meyerhof, ''Shallow foundations,'' Journal of Soil Mechanics and Foundation Division, ASCE, 91(2), 1965, pp. 21–31.
7. G. G. Meyerhof, "General Report: State-of-the-Art of Penetration testing in Countries Outside Europe." Proceedings of the 1st European Symposium on Penetration Testing, Vol. 2.1, 1974pp. 40-48.
8. J. H. Schmertmann, J. D. Hartman, and P. R. Brown, "Improved Strain Influence Factor Diagrams." Journal of the Geotechnical Division, ASCE, Vol. 104, No. GT8, 1978, pp. 1131-1135.
9. P. K. Robertson, and R. G. Campanella, "Liquefaction potential of sands using the CPT," Journal of Geotechnical Engineering, ASCE, 111(3), 1985, pp. 384–403.
10. P.W., Mayne, "Cone Penetration Testing State-of-Practice. State-of-Practice," Transportation Research Board. Synth. Study, NCHRP Project 20-05, Topic 37-14, 2007.
11. J. H. Schmertmann, "Static cone to compute static settlement of spread footings on sand," Journal of Soil Mech. and Foundation Division, ASCE, 96(3), 1970, pp.1011–1043.
12. R. Düzceer, "Observed and predicted settlement of shallow foundation," 2nd International Conference on New Developments in Soil Mechanics and Geotechnical Engineering, Nicosia, North Cyprus. 2009
13. J.B. Herbich, "Coastal Engineering Handbook," McGraw-Hill Professional; 2000.
14. B.M. Das, "Principle of Geotechnical Engineering," 3rd edition. Boston: PWS Kent Publishers. 1994.
15. G. G. Meyerhof, "Penetration Tests and Bearing Capacity of Cohesionless Soils." Journal of the Soil Mechanics Division, ASCE, Vol. 82, SM1, 1956, pp. 1-12.
16. G.G. Meyerhof and A. Fellenius, "Foundation Engineering Manual," (second edition), Canadian Geotechnical Society, 1985.
17. J. L. Briaud and E. Garland, "Loading rate method for pile response in clay." Journal of Geotechnical Engineering, ASCE, 111(3), 1985, pp. 319–335.
18. J. L. Briaud, "Spread Footings in Sand: Load Settlement, Curve Approach," Journal of Geotechnical and Geoenvironmental Engineering, 133(8), 2007, pp. 905–920.
19. J. L. Briaud and R. M. Gibbens "Test and prediction results for five large spread footings on sand," FHWA Prediction Symp. ASCE Spec. Publ. No. 41, ASCE, New York, 1994, pp. 92–128.
20. Eurocode 7 (EN 1997-2), Geotechnical design - Part 2: Ground investigation and testing.
21. L. Wils, W. F. Van Impe., W. Haegeman, and P. O. Van Impe, "Laboratory testing issues related to crushable sands," Proceedings of the 18th International Conference on Soil Mechanics and Geotechnical Engineering, Paris, 2013.
22. S. Eslaamizaad and P. K. Robertson, "Seismic cone penetration test to identify cemented sands," International Proceedings of the 49th Canadian Geotechnical Conference, St. John's, N.L., 23–25. Edited by J.I. Clark. Canadian Geotechnical Society, Richmond, B.C. September 1996, pp. 352–360.

AUTHOR PROFILE

Hossam E A. Ali: Dr. Hossam Eldin Ali has an academic experience of more than 30 years including research and teaching. He is currently an Associate professor at Ain Shams University. Dr. Ali has graduated with Bachelor degree in civil engineering with honor at Ain Shams University in Cairo in 1990 followed by Master of Science at the same university in geotechnical engineering in 1994. He got his PhD in Geotechnical Engineering, at Kansas State University, USA, in 2000 over the research regarding neuronet-based liquefaction potential assessment and stress-strain behavior simulation of sandy soils.

Dr. Ali has more than 30 published journal and conference papers in the field of Geotechnical Engineering, artificial intelligence and pavement design.

He has broad experience in design and analysis of geotechnical systems including Earth dams, Tunnels & underground excavation deep and shallow foundations in soil and rocks, ground improvement, dredging and reclamation works. His involvement in design and construction of reclaimed bodies and marine structures such as artificial islands and ports facilities is remarkable. He has professional Engineer certificate from board of engineering in Ohio, USA and the Egyptian Engineering Syndicate.